Effects of Porphyrin Substituents and Adsorption Conditions on Photovoltaic Properties of Porphyrin-Sensitized TiO2 Cells

Hiroshi Imahori,*,[†,‡,§] Shinya Hayashi,[‡] Hironobu Hayashi,[‡] Akane Oguro,[‡] Seunghun Eu,[‡] Tomokazu Umeyama,[‡] and Yoshihiro Matano[‡]

Institute for Integrated Cell-Material Sciences (iCeMS), Kyoto University, Nishikyo-ku, Kyoto 615-8510, Japan, Department of Molecular Engineering, Graduate School of Engineering, Kyoto University, Nishikyo-ku, Kyoto 615-8510, Japan, and Fukui Institute for Fundamental Chemistry, Kyoto University, 34-4, Takano-Nishihiraki-cho, Sakyo-ku, Kyoto 606-8103, Japan

Received: July 30, 2009; Revised Manuscript Received: August 29, 2009

A series of *meso*-tetraphenylzincporphyrins have been prepared to examine the effects of the porphyrin substituents and adsorption conditions on photovoltaic properties of the porphyrin-sensitized TiO2 cells. The cell performance strongly depended on the linking bridge between the porphyrin core and the TiO2 surface, the bulkiness around the porphyrin core, and the immersing solvents and times for the porphyrin adsorption. In particular, the high cell performance of the porphyrin-sensitized TiO2 cells was achieved when protic solvent (i.e., methanol) and short immersing time (0.5−1 h) were used for the conditions of the dye adsorption on TiO2, which is in sharp contrast with Ru dye-sensitized TiO2 cells. The highest cell performance was obtained with 5-(4-carboxyphenyl)-10,15,20-tris(2,4,6-trimethylphenyl)porphyrinatozinc(II) as a sensitizer and methanol as an immersing solvent with an immersing time of 1 h: a maximal incident photon-to-current efficiency of 76%, a short circuit photocurrent density of 9.4 mA cm^{-2}, an open-circuit voltage of 0.76 V, a fill factor of 0.64, and a power conversion efficiency of 4.6% under standard AM 1.5 sunlight. These results will provide basic and valuable information on the development of dye-sensitized solar cells exhibiting a high performance.

Introduction

Photoinduced electron transfer (ET) processes are of vital importance in versatile biological and chemical systems.[1] For instance, a cascade of photoinduced ET along a well-arranged donor−acceptor array in the photosynthetic reaction center is essential for the conversion of solar energy into chemical energy.[2] A variety of synthetic donor−acceptor systems have been prepared for better understanding of the controlling factors in ET processes.[3−5] In this context, extensive efforts have been devoted to develop interfacial photoinduced ET systems for photochemical and photovoltaic energy conversion,[6−8] including dye-sensitized nanocrystalline metal oxides[9,10] and bulk heterojunction blend films.[11−14] Specifically, Grätzel et al. developed solar cells based on the sensitization of highly porous TiO2 by molecular dyes with power conversion efficiencies (η) of 7−11%, making practical applications feasible.[9]

To date, ruthenium(II) bipyridyl complexes have proven to be the most efficient TiO2 sensitizers.[9,10] Nevertheless, the rather complex molecular structures with multiple binding moieties to the TiO2 surfaces make it difficult to disclose the close relationship between the molecular structure and photovoltaic function. Attempts to employ different kinds of dyes have achieved significant success, but the cell performance is still lower or comparable to that of ruthenium dye-sensitized TiO2 cells.[15−23] Although the substituent effects of molecular dyes relating to bridge influences, electronic coupling, and aggregation on the photochemical and photovoltaic properties have been examined,[23] the relationship between the molecular structure and photovoltaic properties has remained elusive.

For photovoltaic cells with *meso*-tetraphenylporphyrin-sensitized TiO2 electrodes, different incident photon-to-current efficiency (IPCE) and η values have been reported depending on the substituents and adsorption conditions.[17−22] Durrant et al. reported that, despite the differences in redox potential and photophysics between carboxylated porphyrin sensitizers such as **ZnTCPP** and its free-base **H2TCPP** and the ruthenium polypyridyl **N3** dye (Figure 1), the efficiency of electron injection into a conduction band (CB) of TiO2 and the kinetics of electron injection and charge recombination are virtually similar for all these sensitizers.[24] Furthermore, the charge recombination rate between electrons in the CB and oxidized porphyrins is in the range of several milliseconds, which is sufficiently slow to permit the regeneration of the porphyrin ground state by the iodide in the electrolyte.[24] In spite of these observations, porphyrins are known to be inefficient sensitizers compared with ruthenium polypyridyl dyes. As such, the effects of porphyrin substituents and adsorption conditions on the photovoltaic properties of porphyrin-sensitized TiO2 electrodes have not been fully understood.

In this paper, we report the effects of porphyrin substituents and adsorption conditions (i.e., immersing solvent and time) on the photovoltaic properties of porphyrin-sensitized TiO2 cells. 5,10,15,20-Tetraphenylporphyrinatozinc(II) (ZnP) was chosen as a sensitizer, because systematic substituents on the *meso*-phenyl groups allow us to evaluate such effects (Figure 2).[22] One carboxy group is attached on the *meso*-phenyl ring to ensure the single anchorage of the porphyrin molecule on a TiO2 surface where the porphyrin geometry is susceptible to the molecular

* E-mail: imahori@scl.kyoto-u.ac.jp.
† Institute for Integrated Cell-Material Sciences (iCeMS), Kyoto University.
‡ Department of Molecular Engineering, Graduate School of Engineering, Kyoto University.
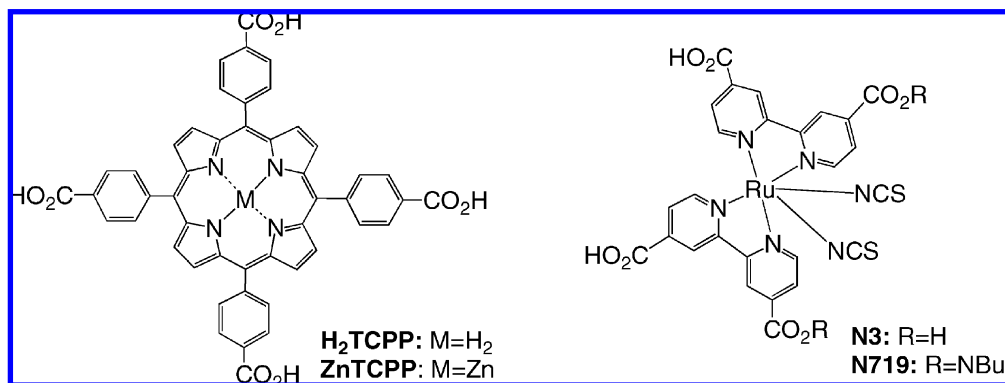§ Fukui Institute for Fundamental Chemistry, Kyoto University.

Properties of Porphyrin-Sensitized TiO₂ Cells

J. Phys. Chem. C, Vol. 113, No. 42, 2009 **18407**

Figure 1. Molecular structures of carboxylated porphyrins and ruthenium polypyridyl dyes.
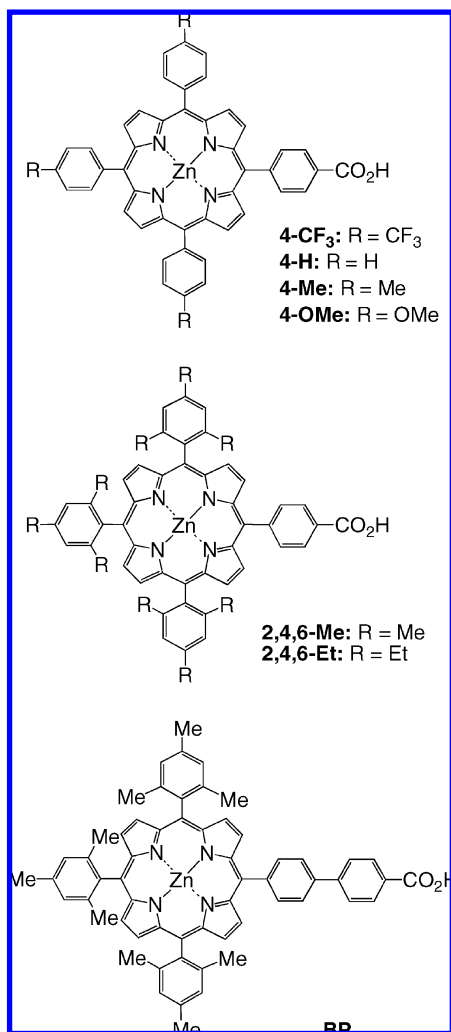

Figure 2. Molecular structures of carboxylated porphyrins used in this study.

structure as well as the adsorption conditions. Therefore, the variations on the molecular structure and the adsorption conditions will have a large impact on molecular packing, geometry, and aggregation of the porphyrin molecules on the TiO₂ electrodes, eventually affecting the photovoltaic properties. The photovoltaic properties are also compared with those of the **N719**-sensitized TiO₂ cell under the same conditions (Figure 1).

Results and Discussion

Synthesis and Characterization. 5,10,15,20-Tetraphenyl-porphyrinatozinc(II)[25−29] compounds bearing a carboxylic group,

4-CF₃, **4-H**,[18b,28] **4-Me**, **4-OMe**,[29] **2,4,6-Me**,[8e,17b,c,22a,f,g] **2,4,6-Et**, and **BP** (Figure 2), were prepared by condensation of pyrrole with the corresponding benzaldehydes in the presence of BF₃·OEt₂, followed by base hydrolysis in a mixture of THF and water and subsequent treatment with zinc acetate. Their molecular structures were verified by ¹H NMR and MALDI-TOF and high-resolution FAB mass spectrometries (see the experimental details in the Supporting Information).

Spectroscopic and Electrochemical Studies. The UV−visible absorption spectra of zincporphyrins used for the photovoltaic measurements were measured in CH₂Cl₂ and the absorption maxima for the Soret and Q bands of the porphyrins are listed in Table 1. For instance, the UV−visible absorption spectrum of **2,4,6-Me** reveals characteristic strong Soret and moderate Q bands (λ_{abs} = 420, 548, 586 nm) (Figure 3, solid line). All porphyrins show approximately the same shape and the peak positions in the Soret region, as well as in the Q bands region. The fluorescence spectra of the porphyrins were also measured in CH₂Cl₂, and the emission maxima are summarized in Table 1. The fluorescence spectrum of **2,4,6-Me** exhibits emission with two peaks (λ_{em} = 595, 645 nm) arising from the porphyrin core (Figure 3, dashed line). The shape and the peak positions of the spectra are analogous for all compounds. These results imply that the electronic structures of the porphyrin core are not perturbed largely by the substituents at the *meso*-phenyl groups.

The one-electron oxidation potentials (E_{ox}) due to the porphyrins are determined by using cyclic voltammetry in CH₂Cl₂ containing 0.1 M *n*-Bu₄NPF₆ as a supporting electrolyte (Table 1). From the absorption, emission, and electrochemical data, the excited state redox potentials ($E_{ox}*$) are approximated by extracting the zero excitation energy ($E_{0−0}$) from the potentials of the ground state couples (Table 1). Driving forces for electron injection (ΔG_{inj}) from the porphyrin excited singlet state to the CB of TiO₂ (−0.5 V vs. NHE)[22] and charge recombination (ΔG_{cr}) between the resulting porphyrin radical cation and the electron in the CB of TiO₂ are determined from the values in Table 1. Note that the corresponding values of **N3** dye are also listed in Table 1 for comparison.[30] Both of the processes are thermodynamically feasible and the difference in the driving forces is virtually negligible for **4-Me**, **2,4,6-Me**, **2,4,6-Et**, and **BP**, whereas a series of the 4-substituted tetraphenylzincporphyrins (**4-CF₃**, **4-H**, **4-OMe**, and **4-Me**) reveals slight difference in the driving forces depending on the electron-donating or -withdrawing substituents.

Film Preparation. Nanoporous films were prepared from colloidal suspension of TiO₂ nanoparticles (P-25) dispersed in distilled water (experimental details are given in the Supporting Information).[22,31] The suspension was deposited on a conducting glass by using the doctor blade technique. The films were

TABLE 1: Optical and Electrochemical Data and Driving Forces for Electron Transfer Processes on TiO$_2$

dye	$\lambda_{abs}{}^a$/nm	$\lambda_{em}{}^b$/nm	$E_{ox}{}^c$/V	$E_{0-0}{}^d$/eV	$E_{ox}^*{}^e$/V	$\Delta G_{inj}{}^f$/eV	$\Delta G_{cr}{}^g$/eV
4-CF$_3$	418, 547, 583	596, 644	1.08	2.10	−1.02	−0.52	−1.58
4-H	418, 547, 583	597, 646	1.03	2.10	−1.07	−0.57	−1.53
4-Me	420, 548, 588	596, 648	0.99	2.10	−1.11	−0.61	−1.49
4-OMe	422, 552, 589	602, 649	1.02	2.08	−1.06	−0.56	−1.52
2,4,6-Me	420, 548, 586	595, 645	1.00	2.10	−1.10	−0.60	−1.50
2,4,6-Et	422, 550, 588	597, 648	1.00	2.09	−1.09	−0.59	−1.50
BP	420, 549, 585	595, 646	0.98	2.10	−1.12	−0.58	−1.48
N3			1.09^h	1.75^h	−0.64^h	−0.14^h	−1.59^h

^{a} Wavelengths for the maxima of Soret and Q bands in CH$_2$Cl$_2$. ^{b} Wavelengths for emission maxima in CH$_2$Cl$_2$ by exciting at the Soret wavelength. ^{c} First oxidation potentials determined by using cyclic voltammetry in CH$_2$Cl$_2$ containing 0.1 M n-Bu$_4$NPF$_6$ as a supporting electrolyte (vs. NHE). ^{d} E_{0-0} values were estimated from the intersection of the absorption and emission spectra. ^{e} Excited state oxidation potentials approximated from E_{ox} and E_{0-0} (vs. NHE). ^{f} Driving forces for electron injection from the porphyrin excited singlet state (E_{ox}^*) to the CB of TiO$_2$ (−0.5 V vs. NHE). ^{g} Driving forces for charge recombination from the CB of TiO$_2$ to the porphyrin radical cation (E_{ox}). ^{h} From ref 30.
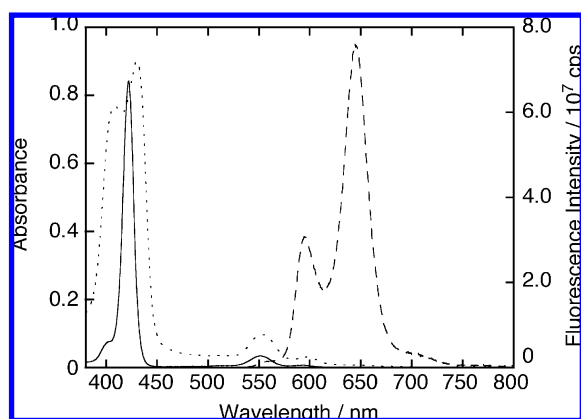

Figure 3. Absorption (2.0 × 10^{-6} M, solid line) and fluorescence (dashed line) spectra of **2,4,6-Me** in CH$_2$Cl$_2$. Absorption spectrum of **2,4,6-Me** on the TiO$_2$ electrode (dotted line) is also shown for comparison. The thickness of the TiO$_2$ electrode was adjusted to be 700−1000 nm to obtain the shape and peak position of the spectra accurately. The porphyrin-modified TiO$_2$ electrodes were obtained from the *tert*-butyl alcohol−acetonitrile mixed (1:1, v/v) solution of **2,4,6-Me** (0.2 mM) for an immersing time of 12 h.

annealed at 673 K for 10 min, followed by similar deposition and annealing (723 K, 2 h) for the 10-μm-thick TiO$_2$ films. The TiO$_2$ electrodes were immersed into various solvents containing 0.2 mM dye at room temperature. Finally, the dye-modified electrodes were rinsed with the same solvent as for the adsorption (denoted as TiO$_2$/ZnP or **N719**). Total amounts of the dyes adsorbed on the TiO$_2$ films were determined by measuring the absorbance of the dyes that were dissolved from the dye-modified TiO$_2$ films into DMF containing 0.1 M NaOH. For instance, taking into account the surface area of P-25 (54 m^2 g^{-1}),[22,31] the porphyrin packing densities (Γ) on the actual surface area are determined to be 1.3 × 10^{-10} mol cm^{-2} for TiO$_2$/**2,4,6-Me** and 1.8 × 10^{-10} mol cm^{-2} for TiO$_2$/**4-H** when **2,4,6-Me** and **4-H** are adsorbed onto the TiO$_2$ surface in *tert*-butyl alcohol−acetonitrile mixture (1:1, v/v) for 12 h, respectively (Table 2). The adsorption conditions are typical for evaluating the cell performance of the **N-719**-sensitized solar cell. Dye molecules bearing carboxylic groups are known to adsorb onto a TiO$_2$ surface, leading to the formation of monolayers on the surface.[9] Assuming that (i) the porphyrin molecule is a rectangular hexahedron and (ii) the porphyrin molecules bearing one carboxylic group are densely packed onto the TiO$_2$ surface to which the carboxylic group binds, the minimum occupied areas of one molecule on the TiO$_2$ surface are calculated to be ca. 140 Å^2 (7 × 20 Å^2) for TiO$_2$/**2,4,6-Me** and ca. 90 Å^2 (5 × 18 Å^2) for TiO$_2$/**4-H**. Accordingly, the Γ

values are estimated to be 1.2 × 10^{-10} mol cm^{-2} for TiO$_2$/**2,4,6-Me** and 1.8 × 10^{-10} mol cm^{-2} for TiO$_2$/**4-H**, which agree well with the experimental values (Table 2). In the case of MeOH as an immersing solvent and the immersing time of 12 h, similar results are obtained for TiO$_2$/**2,4,6-Me** and TiO$_2$/**4-H** (Table 2). Good agreement between the experimental and calculated Γ values in the other types of porphyrins corroborates that porphyrin molecules are densely packed on the TiO$_2$ surface.

Spectroscopic Characterization of Porphyrin Films on TiO$_2$. To gain further insight into the structures of the porphyrin monolayers on the TiO$_2$ surface, UV−visible absorption spectra of the TiO$_2$/**2,4,6-Me** electrode were measured under different adsorption conditions (Figure 3 and Figure S2 in the Supporting Information). The thickness of the TiO$_2$ substrate was adjusted to be 0.7−1.0 μm to obtain the shape and peak position of the whole spectra accurately. The split Soret bands can be attributed to the excitonic interaction between the porphyrins,[22] which is consistent with closely packed monolayers of the porphyrins on the TiO$_2$. The peak positions and the shape of the Soret and Q bands of TiO$_2$/**2,4,6-Me** are slightly different depending on immersing solvents (i.e., *tert*-butyl alcohol−acetonitrile mixture vs. MeOH) and times (i.e., 12 h vs. 1 h), which would affect the photovoltaic properties in the present cell.

Attenuated total reflectance-Fourier transform infrared (ATR-FTIR) spectroscopy is known to be a useful tool for gaining the information on the binding mode of the molecules adsorbed on the TiO$_2$ substrate.[22] In this study, the interpretations for the ATR-FTIR spectra of the porphyrin monolayers are aided by comparison with the FTIR spectra of the corresponding porphyrin powder in a KBr pellet. Figure 4 depicts the FTIR spectra of **2,4,6-Me** measured as a pure solid and the ATR-FTIR spectra of TiO$_2$/**2,4,6-Me** obtained from MeOH as an immersing solvent and the immersing times of 12 and 1 h. The FTIR spectrum of **2,4,6-Me** obtained from a solid sample reveals the characteristic band of ν(C=O) of the carboxylic acid group at around 1700 cm^{-1} (Figure 4a).[16c,e,22,32] This diagnostic for the ν(C=O) disappears for the ATR-FTIR spectra of TiO$_2$/**2,4,6-Me** (Figure 4b,c). The ATR-FTIR spectra of TiO$_2$/**2,4,6-Me** exhibit a marked increase in the symmetric carboxylate band, ν(COO$_s^-$), at around 1400 cm^{-1}.[16c,e,22,32] The disappearance of ν(C=O) and the increased intensities of ν(COO$_s^-$) corroborate that a proton is detached from the carboxylic acid group during the adsorption of the porphyrin on the TiO$_2$ surface, leading to the bidentate binding of the carboxylate group to the TiO$_2$ surface.[33] This is consistent with the previous assignment that a carboxylic acid of analogous porphyrins is bound to a TiO$_2$ surface via a bridging bindentate mode[16c,e] together with the fact that X-ray photoelectron spectroscopy measurement for alike tetraphe-

Properties of Porphyrin-Sensitized TiO$_2$ Cells

J. Phys. Chem. C, Vol. 113, No. 42, 2009 **18409**

TABLE 2: Surface Coverage of Dyes on TiO$_2$

	exptl Γ for different immersing solvent and time/10^{-10} mol cm^{-2}					
electrode	*t*-BuOH:CH$_3$CN (1 h)	*t*-BuOH:CH$_3$CN (12 h)	MeOH (0.5 h)	MeOH (1 h)	MeOH (12 h)	calcd Γ/ 10^{-10} mol cm^{-2}
TiO$_2$/**4-CF$_3$**	1.4	1.3	1.2	1.4	1.3	1.5[a]
TiO$_2$/**4-H**	0.53	1.8	0.29	0.51	1.6	1.8[a]
TiO$_2$/**4-Me**	1.4	1.4	1.5	1.5	1.5	1.6[a]
TiO$_2$/**4-OMe**	1.4	1.6	0.93	1.4	1.5	1.5[a]
TiO$_2$/**2,4,6-Me**	1.0	1.3	0.85	1.2	1.2	1.2[a]
TiO$_2$/**2,4,6-Et**	0.71	0.69	0.72	0.86	0.84	0.78[a]
TiO$_2$/**BP**	1.2	1.1	1.1	1.1	1.2	1.2[a]
TiO$_2$/**N719**	0.42	2.0	0.26	0.36	1.6	1.9

[a] Assuming that the porphyrin molecules bearing one carboxylic group are densely packed onto the TiO$_2$ surface to which the carboxylic acid binds.
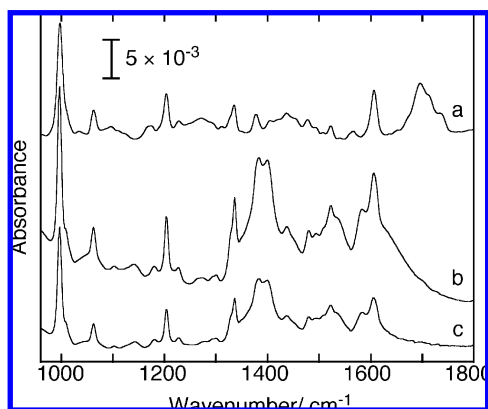

Figure 4. (a) FTIR spectra of **2,4,6-Me** measured as a pure solid. ATR-FTIR spectra of the TiO$_2$/**2,4,6-Me** electrode obtained from MeOH for (b) 12 and (c) 1 h. The thickness of the TiO$_2$ electrode was 10 μm.

nylporphyrin with a carboxylic acid group provided evidence for the bidentate binding of the carboxylate group to the TiO$_2$ surface.[22e]

Photovoltaic Properties of Porphyrin-Sensitized TiO$_2$ Cells. To establish the cell performance of a reference system (i.e., Ru dye) under the present conditions using P-25, first we examined immersing time dependence of the η value for the adsorption of **N719** (0.2 mM) in *tert*-butyl alcohol−acetonitrile mixture (1:1, v/v). Current−voltage characteristics were measured by using a 10-μm-thick TiO$_2$ electrode modified with **N719** and a Pt counter electrode under AM 1.5 conditions (Supporting Information). All experimental values were given as an average from six independent measurements. The η value is increased gradually with increasing the immersing time to reach a maximum η value (η_{max}) of 6.5% for 12 h (Figure 5A). Further increase of the immersing time (>12 h) does not change the η value. The Γ value is also increased with increasing the immersing time to become saturated for 12 h (2.0 × 10^{-10} mol cm^{-2}). The minimum occupied area of one molecule on the TiO$_2$ surface is calculated to be ca. 88 Å^2 (11 × 8 Å^2) for TiO$_2$/**N719**. Accordingly, the Γ value is estimated to be 1.9 × 10^{-10} mol cm^{-2} for TiO$_2$/**N719**, which is consistent with the experimental value (Table 2). The saturated Γ value is comparable to the previously reported Γ value in which Ru dyes are organized on the TiO$_2$ surface as a densely packed monolayer.[9,34] Accordingly, the time profile of the η value correlates well with that of the Γ value. It is noteworthy that the η value optimized for the immersing time (i.e., 12 h) slightly decreases in the order of *tert*-butyl alcohol−acetonitrile mixture (1:1, v/v) (6.5%), CH$_2$Cl$_2$ (6.1%), and MeOH (5.5%), as shown in Figure 5B and
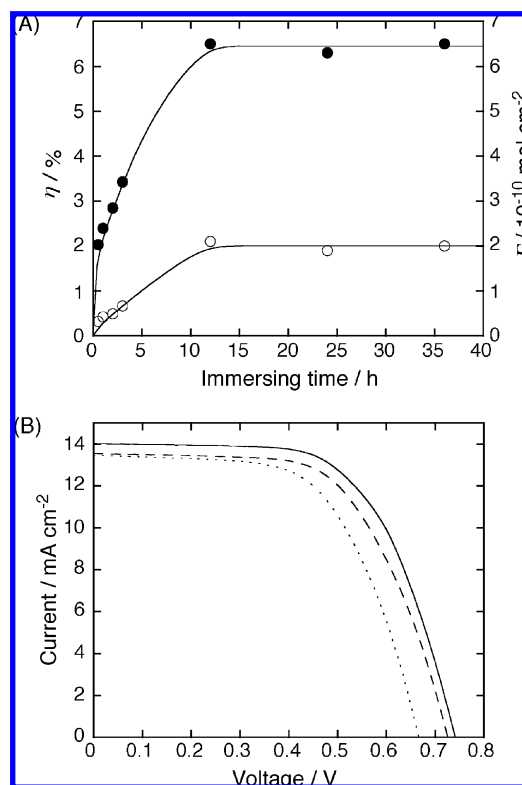

Figure 5. (A) Immersing time profiles of the η value (close circle) and of the surface density (Γ) of the **N719** dye adsorbed on a TiO$_2$ electrode (open circle) in *tert*-butyl alcohol and acetonitrile mixture (1:1, v/v). (B) Current−voltage characteristics of **N719**-sensitized TiO$_2$ cells: (a) *tert*-butyl alcohol and acetonitrile mixture (1:1, v/v), 12 h (solid line, η = 6.5%); (b) CH$_2$Cl$_2$, 12 h (dashed line, η = 6.1%); and (c) MeOH, 12 h (dotted line, η = 5.5%). Conditions: Electrolyte 0.1 M LiI, 0.05 M I$_2$, 0.6 M 2,3-dimethyl-1-propylimidazolium iodide, and 0.5 M 4-*tert*-butylpyridine in acetonitrile; input power AM 1.5 under simulated solar light (100 mW cm^{-2}). For the **N719**-sensitized cell optimized by using P-25, the short-circuit photocurrent density (J_{sc}) of 14.0 mA cm^{-2}, open-circuit photovoltage (V_{oc}) of 0.74 V, and fill factor (ff) of 0.63 yield a power conversion efficiency (η), derived from the equation $\eta = J_{sc} \times V_{oc} \times$ ff, of 6.5%.

Table 3. The cell performance of the **N719**-sensitized cell optimized for the immersing time is listed in Table 3.

Next, we examined photovoltaic properties of the porphyrin-sensitized TiO$_2$ cells using **2,4,6-Me** as a representative example. For the **2,4,6-Me**-sensitized solar cell, the η value displays strong dependency of the immersing solvents (Figure 6), as contrasted with the weak solvent dependence of the **N719**-sensitized TiO$_2$ cell. The cell performance of the **2,4,6-Me**-sensitized cell for the immersing time of 12 h in each solvent is also summarized

TABLE 3: Cell Performance of Dye-Sensitized Solar Cells

cell	solvent	time/h[b]	IPCE (APCE)/%		J_{sc}/mA cm^{-2}	V_{oc}/mV	ff	η/%
			420nm	560nm				
TiO$_2$/**4-CF$_3$**	*t*-BuOH/MeCN[a]	1	53 (53)[d]	44 (48)	6.4	0.68	0.64	2.8
	MeOH	1	58 (58)	43 (45)	6.6	0.67	0.68	3.0
TiO$_2$/**4-H**	*t*-BuOH/MeCN[a]	1	24 (34)	8.0 (31)	3.0	0.60	0.64	1.2
	t-BuOH/MeCN[a]	12	—[c]	—[c]	1.1	0.51	0.54	0.32
	MeOH	1	25 (31)	7.0 (25)	3.1	0.58	0.66	1.2
	MeOH	12	—[c]	—[c]	1.1	0.53	0.58	0.34
TiO$_2$/**4-Me**	*t*-BuOH/MeCN[a]	1	50 (50)	40 (42)	6.9	0.67	0.66	3.0
	MeOH	0.5	62 (62)	46 (47)	8.3	0.68	0.68	3.8
TiO$_2$/**4-OMe**	*t*-BuOH/MeCN[a]	1	60 (60)[d]	34 (37)	6.7	0.67	0.67	3.0
	MeOH	1	65 (65)	42 (44)	8.3	0.66	0.63	3.5
TiO$_2$/**2,4,6-Me**	*t*-BuOH/MeCN[a]	1	63 (63)[d]	52 (56)	7.6	0.69	0.64	3.4
	t-BuOH/MeCN[a]	12	64 (64)	30 (32)	5.0	0.64	0.66	2.1
	EtOH	12	—[c]	—[c]	6.9	0.72	0.65	3.2
	MeOH	1	76 (76)	58 (60)	9.4	0.76	0.64	4.6
	MeOH	12	74 (74)	52 (53)	8.3	0.72	0.62	3.7
	DMF	1	68 (68)[d]	46 (53)	7.1	0.66	0.66	3.1
	DMF	12	—[c]	—[c]	1.7	0.55	0.60	0.55
	CH$_2$Cl$_2$	12	—[c]	—[c]	3.0	0.57	0.67	1.1
TiO$_2$/**2,4,6-Et**	*t*-BuOH/MeCN[a]	1	63 (63)[d]	52 (54)	7.7	0.71	0.61	3.3
	t-BuOH/MeCN[a]	12	—[c]	—[c]	6.0	0.64	0.63	2.4
	MeOH	0.5	76 (76)[d]	52 (54)	8.6	0.69	0.63	3.7
	MeOH	12	—[c]	—[c]	7.1	0.66	0.62	2.9
	DMF	12	—[c]	—[c]	2.3	0.62	0.64	0.91
	CH$_2$Cl$_2$	12	—[c]	—[c]	3.6	0.60	0.66	1.4
TiO$_2$/**BP**	*t*-BuOH/MeCN[a]	1	57 (57)	40 (41)	5.6	0.64	0.66	2.4
	MeOH	1	61 (61)	41 (42)	6.0	0.65	0.66	2.6
TiO$_2$/**N719**	*t*-BuOH/MeCN[a]	12	72[e]		14.0	0.74	0.63	6.5
	MeOH	12	—[c]	—[c]	13.5	0.67	0.61	5.5
	CH$_2$Cl$_2$	12	—[c]	—[c]	13.5	0.73	0.62	6.1

[a] 1:1, v/v. *[b]* Short immersing time giving the highest η value. *[c]* Not measured. *[d]* At 430 nm. *[e]* At 520 nm.
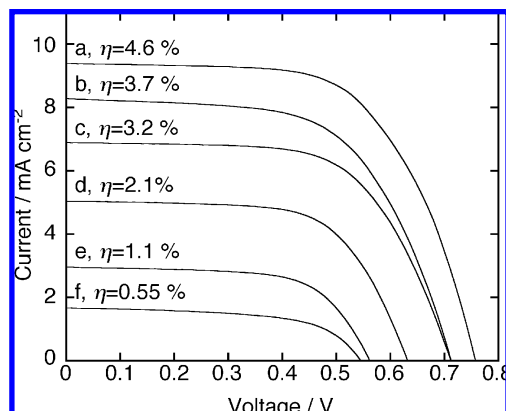

Figure 6. Current−voltage characteristics of **2,4,6-Me**-sensitized TiO$_2$ cells under AM 1.5 conditions. Conditions for the immersing solvent and time: (a) MeOH, 1 h; (b) MeOH, 12 h; (c) EtOH, 12 h; (d) *t*-BuOH−MeCN mixture (1:1, v/v), 12 h; (e) CH$_2$Cl$_2$, 12 h; and (f) DMF, 12 h. Conditions for the photovoltaic measurements: electrolyte 0.1 M LiI, 0.05 M I$_2$, 0.6 M 2,3-dimethyl-1-propylimidazolium iodide, and 0.5 M 4-*tert*-butylpyridine in acetonitrile; input power AM 1.5 under simulated solar light (100 mW cm^{-2}). For the **2,4,6-Me**-sensitized cell optimized with P-25, J_{sc} of 9.4 mA cm^{-2}, V_{oc} of 0.76 V, and ff of 0.64 yield η of 4.6% (curve a).

in Table 3. The η value with **2,4,6-Me** for the immersing time of 12 h increases in the order of DMF (0.55%), CH$_2$Cl$_2$ (1.1%), *tert*-butyl alcohol−acetonitrile mixture (1:1, v/v) (2.1%), EtOH (3.2%), and MeOH (3.7%). The Γ values for **2,4,6-Me** (1.2 × 10^{-10} mol cm^{-2} for EtOH and MeOH, 1.3 × 10^{-10} mol cm^{-2} for *tert*-butyl alcohol−acetonitrile mixture (1:1, v/v)) are virtually the same when the protic solvents are used. On the other hand, they (Γ = 5.3 × 10^{-11} mol cm^{-2} for DMF, 8.7 × 10^{-11} mol cm^{-2} for CH$_2$Cl$_2$) are considerably lower in the case

of the nonprotic solvents. It is concluded that the low porphyrin density on the TiO$_2$ surface for the adsorption in the nonprotic solvents is responsible for the low η value relative to the η value obtained with the adsorption from protic solvents. The high porphyrin density for the adsorption in the protic solvents indicates the significant contribution of the protic solvents for the formation of a densely packed porphyrin monolayer on the TiO$_2$ surface.[22,35] Similar photovoltaic behavior as a function of immersing solvents was reported for the other porphyrins.[22]

To further improve the performance of the **2,4,6-Me**-sensitized TiO$_2$ cell, immersing time dependence of the η value for the adsorption of **2,4,6-Me** was examined in MeOH, which yielded the maximum η value among all the immersing solvents under the same conditions. The η value is increased rapidly with increasing the immersing time to reach a η_{max} value of 4.6% for 1 h and then decreases gradually to reach a constant η value of 3.7% (Figure 7). In accordance with the initial trend, the Γ value also increases rapidly with increasing the immersing time, but levels off at the immersing time of 1 h (Γ = 1.2 × 10^{-10} mol cm^{-2}). Similar behavior of η and Γ values as a function of the immersing time is noted when a mixture of *tert*-butyl alcohol and acetonitrile (1:1, v/v) is used as the immersing solvents for **2,4,6-Me** (Figure S3, Supporting Information) or the other porphyrins that are adsorbed on the TiO$_2$ electrode in MeOH (Figure S4, Supporting Information). It should be noted here that the η_{max} value (4.6%) and the maximum incident photon-to-current efficiency (IPCE) (IPCE$_{max}$ = 76%) of the **2,4,6-Me**-sensitized TiO$_2$ cell are much larger than the corresponding values of the other porphyrin-sensitized TiO$_2$ cells used in this study, exhibiting the highest cell performance when MeOH as the immersing solvent and the immersing time of 0.5 or 1 h are used (Table 3). Furthermore, the η_{max} value of
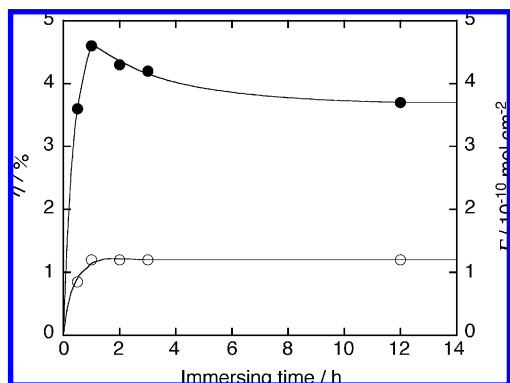
Properties of Porphyrin-Sensitized TiO$_2$ Cells

J. Phys. Chem. C, Vol. 113, No. 42, 2009 **18411**

Figure 7. Immersing time profiles of η value (close circle) and of the surface density (Γ) (open circle) for **2,4,6-Me** adsorbed on the TiO$_2$ electrode in MeOH.
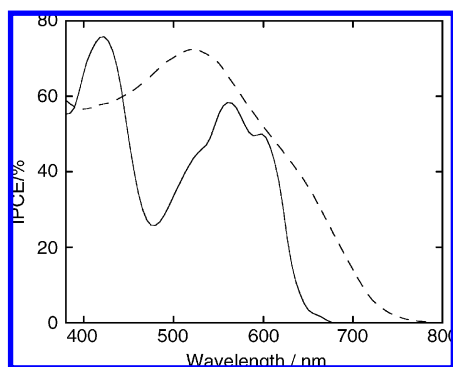

Figure 8. Photocurrent action spectra of (a) **2,4,6-Me**-sensitized solar cell (solid line, MeOH for 1 h) and (b) **N719**-sensitized solar cell (dashed line, *t*-BuOH−MeCN mixture (1:1, v/v) for 12 h) under the optimized conditions: electrolyte 0.1 M LiI, 0.05 M I$_2$, 0.6 M 2,3-dimethyl-1-propylimidazolium iodide, and 0.5 M 4-*tert*-butylpyridine in acetonitrile; input power AM 1.5 under simulated solar light (100 mW cm^{-2}).

the present cell with **2,4,6-Me** is ∼70% that of the ruthenium dye (**N719**)-sensitized TiO$_2$ cell (6.5%) under the present optimized conditions with P-25. The photocurrent action spectrum of the **2,4,6-Me**-sensitized TiO$_2$ cell (Figure 8) is largely similar to the absorption spectrum of **2,4,6-Me** on the TiO$_2$ electrode (Figure 3). Note that integration of the IPCE values for the **2,4,6-Me**-sensitized TiO$_2$ cell with respect to wavenumber is ∼70% that of the **N719**-sensitized TiO$_2$ cell, which parallels the ratio of the η_{max} values in the two cells. The similar ratio (∼70%) reveals that the light-harvesting property of **2,4,6-Me**-sensitized TiO$_2$ cell limits the cell performance. Both device structure and dye are known to have a large impact on the η value of dye-sensitized solar cells.[9,15,16] Grätzel et al. reported the highest η values of 4−7% among porphyrin-sensitized solar cells[16] and of 10−11% for the **N719**-sensitized solar cell[9] under their optimized conditions with use of a TiO$_2$ double layer electrode. Thus, further increase in the cell performance of porphyrin-sensitized TiO$_2$ cells may be possible by improving the device fabrication as well as the light-harvesting property. It should be pointed out that the cell performance of the porphyrin-sensitized TiO$_2$ cells strongly depends on the immersing solvents and the times, which is in marked contrast with Ru dye-sensitized TiO$_2$ cells. The high cell performance in Ru dye-sensitized TiO$_2$ cells may originate from the robust geometry of ruthenium dyes on the TiO$_2$ through more than two anchoring groups, while the rather flexible geometry of the porphyrin on the TiO$_2$ through the single anchoring group may cause the susceptible cell performance,

which is influenced by the porphyrin substituents as well as the adsorption conditions.

Comparison of Photovoltaic Properties. It is intriguing to compare the cell performance of **4-CF$_3$**-, **4-H**-, **4-Me**-, **4-OMe**-, **2,4,6-Me**-, **2,4,6-Et**-, and **BP**-sensitized cells under the same conditions. The results are summarized in Table 3. We consider the following points for the photovoltaic properties.

First, the cell performance of **2,4,6-Me**- and **BP**-sensitized TiO$_2$ cells is compared to evaluate the electronic coupling effect on the photovoltaic properties. When the porphyrins are adsorbed in MeOH for 1 h, the η_{max} and adsorbed photon-to-current efficiency (APCE) values of a **BP** cell (η = 2.6%, IPCE$_{max}$ = 61%) are smaller than those of a **2,4,6-Me** cell (η_{max} = 4.6%, IPCE$_{max}$ = 76%). A similar difference is noted for the comparison of **BP** (η_{max} = 2.4%, IPCE$_{max}$ = 57%) and **2,4,6-Me** cells (η_{max} = 3.4%, IPCE$_{max}$ = 63%) when adsorbed in *tert*-butyl alcohol−acetonitrile mixture (1:1, v/v) for 1 h. Taking into account the same molecular structure of **2,4,6-Me** and **BP** except for the spacer moiety (phenyl vs biphenyl) and full monolayer coverage of the porphyrins on the TiO$_2$ surface, the electronic coupling between the porphyrin and the TiO$_2$ has a large impact on the cell performance. Analogous spacer length dependence of the η value on zincporphyrins with conjugated phenylethylnyl spacers was reported.[18h]

Second, the driving force effects on the photovoltaic properties of **4-CF$_3$**-, **4-OMe**-, **4-H**-, and **4-Me**-sensitized TiO$_2$ cells are evaluated. Under the adsorption conditions exhibiting the highest values (i.e., MeOH for 0.5 or 1 h), the η_{max} and IPCE$_{max}$ values are rather similar for **4-CF$_3$** (η_{max} = 3.0%, IPCE$_{max}$ = 58%), **4-OMe** (η_{max} = 3.5%, IPCE$_{max}$ = 65%), and **4-Me** cells (η_{max} = 3.8%, IPCE$_{max}$ = 62%) except for the case of **4-H** (η_{max} = 1.2%, IPCE$_{max}$ = 25%). A similar trend is observed for the η_{max} values of **4-CF$_3$** (η_{max} = 2.8%), **4-OMe** (η_{max} = 3.0%), **4-H** cell (η_{max} = 1.2%), and **4-Me** cells (η_{max} = 3.0%) when adsorbed in *tert*-butyl alcohol−acetonitrile mixture (1:1, v/v) for 1 h. Although the driving force for electron injection (ΔG_{inj}) from the porphyrin excited singlet state to the CB of the TiO$_2$ electrode increases with introducing the electron-donating substituents (−0.52 eV for **4-CF$_3$**, −0.56 eV for **4-OMe**, −0.57 eV for **4-H**, −0.61 eV for **4-Me**), the η_{max} and IPCE$_{max}$ values are unlikely to correlate with the driving force for the electron injection. The considerably low η_{max} value of the **4-H** cell may be rationalized by the rather low porphyrin density of **4-H** on the TiO$_2$ in comparison to that of the other porphyrins at the short immersing time of 0.5 or 1 h (Table 2). Additionally, a strong aggregation tendency of **4-H** on the TiO$_2$ due to the small steric hindrance also would be responsible for the low η value of the **4-H** cell, taking into account the remarkable decrease in the η value for the long immersing time (Table 3 and Figure S4 in the Supporting Information).

The steric effect on the photovoltaic properties is examined for **4-Me**-, **2,4,6-Me**-, and **2,4,6-Et**-sensitized TiO$_2$ cells. For example, under the adsorption conditions exhibiting the highest values (i.e., MeOH for 0.5 or 1 h), the η_{max} and IPCE$_{max}$ values of the **2,4,6-Me** cell (η_{max} = 4.6%, IPCE$_{max}$ = 76%) are larger than those of the **4-Me** (η_{max} = 3.8%, IPCE$_{max}$ = 62%) and **2,4,6-Et** cells (η_{max} = 3.7%; IPCE$_{max}$ = 76%). Similar results are obtained for the η_{max} values of **4-Me** (η_{max} = 3.0%), **2,4,6-Me** (η_{max} = 3.4%), and **2,4,6-Et** cells (η_{max} = 3.3%) when adsorbed in *tert*-butyl alcohol−acetonitrile mixture (1:1, v/v) for 0.5−1 h. Large steric repulsion between the *o*-methyl or -ethyl substituents and the porphyrin ring in **2,4,6-Me** and **2,4,6-Et** results in orthogonal orientation of the phenyl groups against the porphyrin ring, making large bulkiness around the porphyrin

rings. In such a case, even in the densely packed state, the rather well-separated porphyrin cores of **2,4,6-Me** would reduce the intermolecular interaction between the porphyrins on the TiO$_2$ surface, thereby leading to a decrease of radiationless processes from the porphyrin excited singlet state and a subsequent increase of the electron injection efficiency, in turn an increase of the η value with use of **2,4,6-Me** relative to that of **4-Me**.[36] The decrease in the η value of the **2,4,6-Et** cell relative to that of the **2,4,6-Me** cell may be caused by the small porphyrin density ($\Gamma = (0.71-0.72) \times 10^{-10}$ mol cm^{-2}) on the TiO$_2$ electrode compared with the Γ value ($\Gamma = (1.0-1.2) \times 10^{-10}$ mol cm^{-2}) of **2,4,6-Me** on the TiO$_2$ electrode as the result of the difference in the sizes of ethyl and methyl groups.

Finally, the photovoltaic properties are investigated as a function of the adsorption conditions (i.e., immersing solvent and immersing time). For all porphyrins with an increase in the immersing time, the η value is increased rapidly to reach the maximum for 0.5−1 h and then decreased. Such behavior may be rationalized by an increase of the porphyrin aggregation with increasing the immersing time. Despite similar full monolayer coverage of the porphyrins, the cell performances of the porphyrin-sensitized TiO$_2$ electrodes are in the order of *tert*-butyl alcohol−acetonitrile < EtOH < MeOH as an immersing solvent. Although the reason is not clear at present, protic solvents may involve the adsorption process of the porphyrin on the TiO$_2$ surface, altering the binding mode and geometry of the porphyrin on the TiO$_2$ surface.[35]

Conclusions

We have systematically examined the effects of porphyrin substituents and adsorption conditions on the photovoltaic properties of the porphyrin-sensitized TiO$_2$ cells for the first time. The cell performance of the porphyrin-sensitized TiO$_2$ cells was affected greatly by the steric bulkiness around the porphyrin, the electronic coupling between the porphyrin core and the TiO$_2$ surface, the immersing solvent, and the immersing time. In particular, the high cell performance of the porphyrin-sensitized TiO$_2$ cells was realized when protic solvent (i.e., methanol) and short immersing time (0.5−1 h) were used for the conditions of the dye adsorption on TiO$_2$. This unique behavior is in marked contrast with little dependence of the cell performance on Ru dye-sensitized TiO$_2$ cells as a function of the immersing solvent and time. The TiO$_2$ electrode cell with 5-(4-carboxyphenyl)-10,15,20-tris(2,4,6-trimethylphenyl)porphyrinatozinc(II) as a sensitizer exhibited the maximum cell performance: IPCE value of 76%, short circuit photocurrent density of 9.4 mA cm^{-2}, open circuit voltage of 0.76 V, fill factor of 0.64, and power conversion efficiency of 4.6% under standard AM 1.5 sunlight. These results will provide basic and important information on the development of dye-sensitized solar cells with high performance.

Supporting Information Available: Synthesis and experimental details, UV−visible absorption spectra of TiO$_2$/**2,4,6-Me** electrodes prepared under different conditions, immersing time profiles of cell performance and porphyrin density of TiO$_2$/**2,4,6-Me** electrodes prepared from *tert*-butyl alcohol−acetonitrile mixture, and immersing time profiles of cell performance and porphyrin density of TiO$_2$/**4-H** electrodes prepared from MeOH. This material is available free of charge via the Internet at http://pubs.acs.org.

References and Notes

(1) *Electron Transfer in Chemistry*; Balzani, V., Ed.; Wiley-VCH: Weinheim, Germany, 2001.

(2) (a) *The Photosynthetic Reaction Center*; Deisenhofer, J., Norris, J. R., Eds.; Academic Press: San Diego, CA, 1993. (b) *Anoxygenic Photosynthetic Bacteria*; Blankenship, R. E., Madigan, M. T., Bauer, C. E., Eds.; Kluwer Academic Publishing: Dordrecht, The Netherlands, 1995.

(3) (a) Closs, G. L.; Miller, J. R. *Science* **1988**, *240*, 440. (b) Wasielewski, M. R. *Chem. Rev.* **1992**, *92*, 435. (c) Gust, D.; Moore, T. A.; Moore, A. L. *Acc. Chem. Res.* **1993**, *26*, 198. (d) Kurreck, H.; Huber, M. *Angew. Chem., Int. Ed.* **1995**, *34*, 849. (e) Gust, D.; Moore, T. A.; Moore, A. L. *Acc. Chem. Res.* **2001**, *34*, 40.

(4) (a) Harriman, A.; Sauvage, J.-P. *Chem. Soc. Rev.* **1996**, *26*, 41. (b) Paddon-Row, M. N. *Acc. Chem. Res.* **1994**, *27*, 18. (c) Verhoeven, J. W. *Adv. Chem. Phys.* **1999**, *106*, 603. (d) Osuka, A.; Mataga, N.; Okada, T. *Pure Appl. Chem.* **1997**, *69*, 797. (e) Sun, L.; Hammarström, L.; Åkermark, B.; Styring, S. *Chem. Soc. Rev.* **2001**, *30*, 36.

(5) (a) Imahori, H.; Sakata, Y. *Adv. Mater.* **1997**, *9*, 537. (b) Imahori, H.; Sakata, Y. *Eur. J. Org. Chem.* **1999**, 2445. (c) Guldi, D. M. *Chem. Commun.* **2000**, 321. (d) Imahori, H.; Mori, Y.; Matano, Y. *J. Photochem. Photobiol. C* **2003**, *4*, 51. (e) Imahori, H. *Org. Biomol. Chem.* **2004**, *2*, 1425. (f) Imahori, H. *Bull. Chem. Soc. Jpn.* **2007**, *80*, 621.

(6) (a) *Organic Photovoltaics*; Sun, S. S., Sariciftci, N. S., Eds.; CRC: Boca Raton, FL, 2005. (b) *Organic Photovoltaics*; Brabec, C. J., Dyakonov, V., Parisi, J., Sariciftci, N. S., Eds.; Springer: Berlin, Germany, 2003. (c) *Organic Photovoltaics*; Brabec, C., Dyakonov, V., Scherf, U., Eds.; Wiley-VCH: Weinheim, Germany, 2008.

(7) (a) Tang, C. W. *Appl. Phys. Lett.* **1986**, *48*, 183. (b) Peumans, P.; Yakimov, A.; Forrest, S. R. *J. Appl. Phys.* **2003**, *93*, 3693. (c) Gregg, B. A. *J. Phys. Chem. B* **2003**, *107*, 4688. (d) Coakley, K. M.; McGehee, M. D. *Chem. Mater.* **2004**, *16*, 4533.

(8) (a) Imahori, H.; Fukuzumi, S. *Adv. Funct. Mater.* **2004**, *14*, 525. (b) Imahori, H. *J. Mater. Chem.* **2007**, *17*, 31. (c) Umeyama, T.; Imahori, H. *Energy Environ. Sci.* **2008**, *1*, 120. (d) Imahori, H.; Umeyama, T. *J. Phys. Chem. C* **2009**, *113*, 9029. (e) Imahori, H.; Umeyama, T.; Ito, S. *Acc. Chem. Res.* DOI: 10.1021/ar900034t. Published Online: May 1, 2009.

(9) (a) Hagfeldt, A.; Grätzel, M. *Chem. Rev.* **1995**, *95*, 49. (b) Hagfeldt, A.; Grätzel, M. *Acc. Chem. Res.* **2000**, *33*, 269. (c) Grätzel, M. *Nature* **2001**, *414*, 338. (d) Bignozzi, C. A.; Argazzi, R.; Kleverlaan, C. J. *Chem. Soc. Rev.* **2000**, *29*, 87. (e) Lewis, N. S. *Inorg. Chem.* **2005**, *44*, 6900. (f) Durrant, J. R.; Haque, S. A.; Palomares, E. J. *Chem. Commun.* **2006**, 3279. (g) Robertson, N. *Angew. Chem., Int. Ed.* **2006**, *45*, 2338. (h) Mishra, A.; Fischer, M. K. R.; Bäuerle, P. *Angew. Chem., Int. Ed.* **2009**, *48*, 2474.

(10) (a) Hirata, N.; Lagref, J.-J.; Palomares, E. J.; Durrant, J. R.; Nazeeruddin, M. K.; Grätzel, M.; Di Censo, D. *Chem.—Eur. J.* **2004**, *10*, 595. (b) Piotrowiak, P.; Galoppini, E.; Wei, Q.; Meyer, G. J.; Wiewior, P. *J. Am. Chem. Soc.* **2003**, *125*, 5278. (c) Kamat, P. V.; Haria, M.; Hotchandani, S. *J. Phys. Chem. B* **2004**, *108*, 5166. (d) Huang, S. Y.; Schlichthörl, G.; Nozik, A. J.; Grätzel, M.; Frank, A. J. *J. Phys. Chem. B* **1997**, *101*, 2576.

(11) (a) Yu, G.; Gao, J.; Hummelen, J. C.; Wudl, F.; Heeger, A. J. *Science* **1995**, *270*, 1789. (b) Padinger, F.; Rittberger, R. S.; Sariciftci, N. S. *Adv. Funct. Mater.* **2003**, *13*, 85. (c) Wienk, M. M.; Kroon, J. M.; Verhees, W. J. H.; Knol, J.; Hummelen, J. C.; van Hal, P. A.; Janssen, R. A. J. *Angew. Chem., Ind. Ed.* **2003**, *42*, 3371. (d) Ma, W.; Yang, C.; Gong, X.; Lee, K.; Heeger, A. J. *Adv. Funct. Mater.* **2005**, *15*, 1617. (e) Scharber, M. C.; Mühlbacher, D.; Koppe, M.; Denk, P.; Waldauf, C.; Heeger, A. J.; Brabec, C. J. *Adv. Mater.* **2006**, *18*, 789. (f) Kim, Y.; Lee, K.; Coates, N. E.; Moses, D.; Nguyen, T.-Q.; Dante, M.; Heeger, A. J. *Science* **2007**, *317*, 222. (g) Hou, J.; Chen, H.-Y.; Zhang, S.; Li, G.; Yang, Y. *J. Am. Chem. Soc.* **2008**, *130*, 16144. (h) Liang, Y.; Feng, D.; Wu, Y.; Tsai, S.-T.; Li, G.; Ray, C.; Yu, L. *J. Am. Chem. Soc.* **2009**, *131*, 7792. (i) Park, S. H.; Roy, A.; Beaupre, S.; Cho, S.; Coates, N.; Moon, J. S.; Moses, D.; Leclerc, M.; Lee, K.; Heeger, A. J. *Nat. Photonics* **2009**, *3*, 297.

(12) (a) Halls, J. J. M.; Walsh, C. A.; Greenham, N. C.; Marseglia, E. A.; Friend, R. H.; Moratti, S. C.; Holmes, A. B. *Nature* **1995**, *376*, 498. (b) Schmidt-Mende, L.; Fechtenkötter, A.; Müllen, K.; Moons, E.; Friend, R. H.; MacKenzie, J. D. *Science* **2001**, *293*, 1119. (c) Nierengarten, J.-F. *New J. Chem.* **2004**, *28*, 1177.

(13) (a) Hiramoto, M.; Fujiwara, H.; Yokoyama, M. *Appl. Phys. Lett.* **1991**, *58*, 1062. (b) Tsuzuki, T.; Shirota, Y.; Rostalski, J.; Meissner, D. *Sol. Energy Mater. Sol. Cells* **2000**, *61*, 1. (c) Xue, J.; Uchida, S.; Rand,

Properties of Porphyrin-Sensitized TiO$_2$ Cells

J. Phys. Chem. C, Vol. 113, No. 42, 2009 **18413**

B. P.; Forrest, S. R. *Appl. Phys. Lett.* **2004**, *84*, 3013. (d) Xue, J.; Rand, B. P.; Uchida, S.; Forrest, S. R. *Adv. Mater.* **2005**, *17*, 66.

(14) (a) Huynh, W. U.; Dittmer, J. J.; Alivisatos, A. P. *Science* **2002**, *295*, 2425. (b) Liu, J.; Tanaka, T.; Sivula, K.; Alivisatos, A. P.; Fréchet, J. M. J. *J. Am. Chem. Soc.* **2004**, *126*, 6550.

(15) (a) Hara, K.; Kurashige, M.; Dan-oh, Y.; Kasada, C.; Shinpo, A.; Suga, S.; Sayama, K.; Arakawa, H. *New J. Chem.* **2003**, *27*, 783. (b) Horiuchi, T.; Miura, H.; Sumioka, K.; Uchida, S. *J. Am. Chem. Soc.* **2004**, *126*, 12218. (c) Kitamura, T.; Ikeda, M.; Shigaki, K.; Inoue, T.; Anderson, N. A.; Ai, X.; Lian, T. Q.; Yanagida, S. *Chem. Mater.* **2004**, *16*, 1806. (d) Schmidt-Mende, L.; Bach, U.; Humphry-Baker, R.; Horiuchi, T.; Miura, H.; Ito, S.; Uchida, S.; Grätzel, M. *Adv. Mater.* **2005**, *17*, 813. (e) Wang, Z. S.; Hara, K.; Dan-Oh, Y.; Kasada, C.; Shinpo, A.; Suga, S.; Arakawa, H.; Sugihara, H. *J. Phys. Chem. B* **2005**, *109*, 3907. (f) Hara, K.; Sato, T.; Katoh, R.; Furube, A.; Yoshihara, T.; Murai, M.; Kurashige, M.; Ito, S.; Shinpo, A.; Suga, S.; Arakawa, H. *Adv. Funct. Mater.* **2005**, *15*, 246. (g) Koumura, N.; Wang, Z.-S.; Mori, S.; Miyashita, M.; Suzuki, E.; Hara, K. *J. Am. Chem. Soc.* **2006**, *128*, 14256. (h) Kim, S.; Lee, J. K.; Kang, S. O.; Ko, J.; Yum, J.-H.; Fantacci, S.; De Angelis, F.; Di Censo, D.; Nazeeruddin, M. K.; Grätzel, M. *J. Am. Chem. Soc.* **2007**, *128*, 16701. (i) Hwang, S.; Lee, J. H.; Park, C.; Lee, H.; Kim, C.; Park, C.; Lee, M.-H.; Lee, W.; Park, J.; Kim, K.; Park, N.-G.; Kim, C. *Chem. Commun.* **2007**, 4887. (j) Ito, S.; Miura, H.; Uchida, S.; Takata, M.; Sumioka, K.; Liska, P.; Comte, P.; Péchy, P.; Grätzel, M. *Chem. Commun.* **2008**, 5194. (k) Choi, H.; Baik, C.; Kang, S. O.; Ko, J.; Kang, M.-S.; Nazeeruddin, M. K.; Grätzel, M. *Angew. Chem., Int. Ed.* **2008**, *47*, 327. (l) Zhang, G.; Bala, H.; Cheng, Y.; Shi, D.; Lv, X.; Yu, Q.; Wang, P. *Chem. Commun.* **2009**, 2198.

(16) (a) Kay, A.; Grätzel, M. *J. Phys. Chem.* **1993**, *97*, 6272. (b) Campbell, W. M.; Burrell, A. K.; Officer, D. L.; Jolley, K. W. *Coord. Chem. Rev.* **2004**, *248*, 1363. (c) Nazeeruddin, M. K.; Humphry-Baker, R.; Officer, D. L.; Campbell, W. M.; Burrell, A. K.; Grätzel, M. *Langmuir* **2004**, *20*, 6514. (d) Schmidt-Mende, L.; Cambell, W. M.; Wang, Q.; Jolley, K. W.; Officer, D. L.; Nazeeruddin, M. K.; Grätzel, M. *ChemPhysChem* **2005**, *6*, 1253. (e) Wang, Q.; Campbell, W. M.; Bomfantani, E. E.; Jolley, K. W.; Officier, D. L.; Walsh, P. J.; Gordon, K.; Humphery-Baker, R.; Nazeeruddin, M. K.; Grätzel, M. *J. Phys. Chem. B* **2005**, *109*, 15397. (f) Campbell, W. M.; Jolley, K. W.; Wagner, P.; Wagner, K.; Walsh, P. J.; Gordon, K. C.; Schmidt-Mende, L.; Nazeeruddin, M. K.; Wang, Q.; Grätzel, M.; Officer, D. L. *J. Phys. Chem. C* **2007**, *111*, 11760.

(17) (a) Cherian, S.; Wamser, C. C. *J. Phys. Chem. B* **2000**, *104*, 3624. (b) Watson, D. F.; Marton, A.; Stux, A. M.; Meyer, G. J. *J. Phys. Chem. B* **2003**, *107*, 10971. (c) Watson, D. F.; Marton, A.; Stux, A. M.; Meyer, G. J. *J. Phys. Chem. B* **2004**, *108*, 11680. (d) Rochford, J.; Chu, D.; Hagfeldt, A.; Galoppini, E. *J. Am. Chem. Soc.* **2007**, *129*, 4655. (e) Stromberg, J. R.; Marton, A.; Kee, H. L.; Kirmaier, C.; Diers, J. R.; Muthiah, C.; Taniguchi, M.; Lindsey, J. S.; Bocian, D. F.; Meyer, G. J.; Holten, D. *J. Phys. Chem. C* **2007**, *111*, 15464. (f) Rochford, J.; Galoppini, E. *Langmuir* **2008**, *24*, 5366.

(18) (a) Boschloo, G. K.; Goossens, A. *J. Phys. Chem.* **1996**, *100*, 19489. (b) Koehorst, R. B. M.; Boschloo, G. K.; Savenije, T. J.; Goossens, A.; Schaafsma, T. J. *J. Phys. Chem. B* **2000**, *104*, 2371. (c) Clifford, J. N.; Yahioglu, G.; Milgrom, L. R.; Durrant, J. R. *Chem. Commun.* **2002**, 1260. (d) Odobel, F.; Blart, E.; Lagrée, M.; Villiera, M.; Boujtita, H.; El Murr, N.; Caramori, S.; Bignozzi, C. A. *J. Mater. Chem.* **2003**, *13*, 502. (e) Jasieniak, J.; Johnston, M.; Waclawik, E. R. *J. Phys. Chem. B* **2004**, *108*, 12962. (f) Lee, C.-W.; Lu, H.-P.; Lan, C.-M.; Huang, Y.-L.; Linag, Y.-R.; Yen, W.-N.; Liu, Y.-C.; Lin, Y.-S.; Diau, E. W.-G.; Yeh, C.-Y. *Chem.—Eur. J.* **2009**, *15*, 1403. (g) Liu, Y. J.; Xiang, N.; Feng, X. M.; Shen, P.; Zhou, W. P.; Weng, C.; Zhao, B.; Tan, S. T. *Chem. Commun.* **2009**, 2499. (h) Lin, C. Y.; Lo, C. F.; Luo, L.; Lu, H. P.; Hung, C. S.; Diau, E. W.-G. *J. Phys. Chem. C* **2009**, *113*, 755.

(19) (a) Ma, T. L.; Inoue, K.; Yao, K.; Noma, H.; Shuji, T.; Abe, E.; Yu, J. H.; Wang, X. S.; Zhang, B. W. *J. Electroanal. Chem.* **2002**, *537*, 31. (b) Ma, T. L.; Inoue, K.; Noma, H.; Yao, K.; Abe, E. *J. Photochem. Photobiol. A* **2002**, *151*, 207. (c) Hasobe, T.; Fukuzumi, S.; Hattori, S.; Kamat, P. V. *Chem. Asian J.* **2007**, *2*, 265. (d) Kamat, P. V. *J. Phys. Chem. C* **2007**, *111*, 2834. (e) Hasobe, T.; Hattroi, S.; Kamat, P. V.; Fukuzumi, S. *Tetrahedron* **2006**, *62*, 1937. (f) Wang, X.-F.; Zhan, C.-H.; Maoka, T.; Wada, Y.; Koyama, Y. *Chem. Phys. Lett.* **2007**, *447*, 79. (g) Wang, X. F.; Kitao, O.; Zhou, H. S.; Tamiaki, H.; Sasaki, S. *J. Phys. Chem. C* **2009**, *113*, 7954. (h) Park, J. K.; Lee, H. R.; Chen, J.; Shinokubo, H.; Osuka, A.; Kim, D. *J. Phys. Chem. C* **2008**, *112*, 16691.

(20) (a) Fungo, F.; Otero, L. A.; Sereno, L.; Silber, J. J.; Durantini, E. N. *J. Mater. Chem.* **2000**, *10*, 645. (b) Brune, A.; Jeong, G.; Liddell, P. A.; Sotomura, T.; Moore, T. A.; Moore, A. L.; Gust, D. *Langmuir* **2004**, *20*, 8366. (c) Huijser, A.; Marek, P. L.; Savenije, T. J.; Siebbeles, L. D. A.; Scherer, T.; Hauschild, R.; Szmytkowski, J.; Kalt, H.; Hahn, H.; Balaban, T. S. *J. Phys. Chem. C* **2007**, *111*, 11726.

(21) (a) He, J.; Benkö, G.; Korodi, F.; Polívka, T.; Lomoth, R.; Åkermark, B.; Sun, L.; Hagfeldt, A.; Sundström, V. *J. Am. Chem. Soc.*

2002, *124*, 4922. (b) Reddy, P. Y.; Giribabu, L.; Lyness, C.; Snaith, H. J.; Vijaykumar, C.; Chandrasekharam, M.; Lakshmikantam, M.; Yum, J.-H.; Kalyanasundaram, K.; Grätzel, M.; Nazeeruddin, M. K. *Angew. Chem., Int. Ed.* **2007**, *46*, 373. (c) Cíd, J.-J.; Yum, J.-H.; Jang, S.-R.; Nazeeruddin, M. K.; Martínez-Ferrero, E.; Palomares, E. J.; Ko, J.; Grätzel, M.; Torres, T. *Angew. Chem., Int. Ed.* **2007**, *46*, 8358. (d) Eu, S.; Katoh, T.; Umeyama, T.; Matano, Y.; Imahori, H. *Dalton Trans.* **2008**, 5476. (e) Cid, J.-J.; Garcia-Iglesias, M.; Yum, J.-M.; Forneli, A.; Albero, J.; Martinez-Ferrero, E.; Vazquez, P.; Grätzel, M.; Nazeeruddin, M. K.; Palomares, E.; Torres, T. *Chem.—Eur. J.* **2009**, *15*, 5130.

(22) (a) Imahori, H.; Hayashi, S.; Umeyama, T.; Eu, S.; Oguro, A.; Kang, S.; Matano, Y.; Shishido, T.; Ngamsinlapasathian, S.; Yoshikawa, S. *Langmuir* **2006**, *22*, 11405. (b) Eu, S.; Hayashi, S.; Umeyama, T.; Oguro, A.; Kawasaki, M.; Kadota, N.; Matano, Y.; Imahori, H. *J. Phys. Chem. C* **2007**, *111*, 2777. (c) Tanaka, M.; Hayashi, S.; Eu, S.; Umeyama, T.; Matano, Y.; Imahori, H. *Chem. Commun.* **2007**, 2069. (d) Kira, A.; Tanaka, M.; Umeyama, T.; Matano, Y.; Li, G.; Ye, S.; Isosomppi, M.; Tkachenko, N. V.; Lemmetyinen, H.; Imahori, H. *J. Phys. Chem. C* **2007**, *111*, 13618. (e) Eu, S.; Hayashi, S.; Umeyama, T.; Matano, Y.; Araki, Y.; Imahori, H. *J. Phys. Chem. C* **2008**, *112*, 4396. (f) Hayashi, S.; Matsubara, Y.; Eu, S.; Hayashi, H.; Umeyama, T.; Matano, Y.; Imahori, H. *Chem. Lett.* **2008**, *37*, 846. (g) Hayashi, S.; Tanaka, M.; Hayashi, H.; Eu, S.; Umeyama, T.; Matano, Y.; Araki, Y.; Imahori, H. *J. Phys. Chem. C* **2008**, *112*, 15576. (h) Kira, A.; Umeyama, T.; Matano, Y.; Yoshida, K.; Isoda, S.; Park, J. K.; Kim, D.; Imahori, H. *J. Am. Chem. Soc.* **2009**, *131*, 3198. (i) Hayashi, H.; Kira, A.; Umeyama, T.; Matano, Y.; Charoensirithavorn, P.; Sagawa, T.; Yoshikawa, S.; Tkachenko, N. V.; Lemmetyinen, H.; Imahori, H. *J. Phys. Chem. C* **2009**, *113*, 10819.

(23) (a) Persson, P.; Lundqvist, M. J.; Ernstorfer, R.; Goddard, W. A., III; Willig, F. *J. Chem. Theory Comput.* **2006**, *2*, 441. (b) Anderson, N. A.; Ai, X.; Chen, D.; Mohler, D.; Lian, T. *J. Phys. Chem. B* **2003**, *107*, 14231. (c) Wang, D.; Mendelsohn, R.; Galoppini, E.; Hoertz, P. G.; Carlisle, R. A.; Meyer, G. J. *J. Phys. Chem. B* **2004**, *108*, 16642. (d) Kilså, K.; Mayo, E. I.; Kuciauskas, D.; Villahermosa; Lewis, N. S.; Winkler, J. R.; Gray, H. B. *J. Phys. Chem. A* **2003**, *107*, 3379. (e) Hoertz, P. G.; Carlisle, R. A.; Meyer, G. J.; Wang, D.; Piotrowiak, P.; Galoppini, E. *Nano Lett.* **2003**, *3*, 325.

(24) (a) Tachibana, Y.; Haque, S. A.; Mercer, I. P.; Durrant, J. R.; Klug, D. R. *J. Phys. Chem. B* **2000**, *104*, 1198. (b) Clifford, J. N.; Palomares, E. J.; Nazeeruddin, M. K.; Grätzel, M.; Nelson, J.; Li, X.; Long, N. J.; Durrant, J. R. *J. Am. Chem. Soc.* **2004**, *126*, 5225.

(25) Luo, C.; Guldi, D. M.; Imahori, H.; Tamaki, K.; Sakata, Y. *J. Am. Chem. Soc.* **2000**, *122*, 6535.

(26) Fuson, R. C.; Horning, E. C.; Rowland, S. P.; Ward, M. L.; Barnes, R. P. *Org. Synth.* **1943**, *23*, 57.

(27) Blettner, C. G.; Konig, W. A.; Stenzel, W.; Schotten, T. *Synlett* **1998**, 295.

(28) Harada, A.; Shiotsuki, K.; Fukushima, H.; Yamaguchi, H.; Kamachi, M. *Inorg. Chem.* **1995**, *34*, 1070.

(29) Zaoying, L.; Jianglin, L.; Cong, L.; Wei, X. *Synth. Commun.* **2000**, *30*, 917.

(30) Nazeeruddin, M. K.; Kay, A.; Rodicio, I.; Humphry-Baker, R.; Müller, E.; Liska, P.; Vlachopoulos, N.; Grätzel, M. *J. Am. Chem. Soc.* **1993**, *115*, 6382.

(31) Nakade, S.; Matsuda, M.; Kambe, S.; Saito, Y.; Kitamura, T.; Sakata, T.; Wada, Y.; Mori, H.; Yanagida, S. *J. Phys. Chem. B* **2002**, *106*, 10004.

(32) *Spectrometric Identification of Organic Compounds*; Silverstein, R. M.; Bassler, G. C., Morrill, T. C., Eds.; John Wiley & Sons: New York, 1991.

(33) Although the ATR-FTIR spectra of the TiO$_2$/**2,4,6-Me** exhibited new bands at 1500−1600 cm^{-1}, we could not assign these bands owing to the complex molecular structure of the porphyrin.

(34) Shklover, V.; Nazeeruddin, M. K.; Zakeeruddin, S. M.; Barbé, C.; Kay, A.; Haibach, T.; Steurer, W.; Hermann, R.; Nissen, H.-U.; Grätzel, M. *Chem. Mater.* **1997**, *9*, 430.

(35) MeOH molecules are known to adsorb onto a TiO$_2$ surface. There are two modes of the MeOH adsorption, molecular physisorption and dissociative chemisorption. Thus, the protic solvents may influence the adsorption and geometry of the porphyrins on the TiO$_2$ surface. (a) Wang, C.-y.; Groenzin, H.; Shultz, M. J. *J. Phys. Chem. B* **2004**, *108*, 265. (b) Wang, C.-y.; Groenzin, H.; Shultz, M. J. *J. Am. Chem. Soc.* **2005**, *127*, 9736.

(36) Addition of chenodeoxycholic acid (0.2 mM) as an inhibitor of dye aggregation to MeOH solution of **2,4,6-Me** for adsorption onto the TiO$_2$ surface led to a virtually same η value (4.4% vs. 4.6%) for the immersing time of 1 h, while the long immersing time (12 h) results in a slight increase of the η value (4.1% vs. 3.7%).